Malaysian Journal of Chemistry, 2026, Vol. 28(2), 306-318
(Special Issue: *1st International Conference on Chemical and Energy Engineering 2025, ICChEE2025*)

Ultrasonication-Assisted Synthesis of PANI–SiO_2 Nanocomposites for High-Performance Humidity Sensors

Tinghao Xie[1], Anis Farhana Abdul Rahman[1], Aznizam Abu Bakar[2] and Agus Arsad[1]*
[1]UTM-MPRC Institute of Oil & Gas, 81310 Johor Bahru, Malaysia
[2]Faculty of Chemical and Energy Engineering, Universiti Teknologi Malaysia, 81310 Johor Bahru, Malaysia
*Corresponding author (e-mail: agus@utm.my)

Polyaniline–silica (PANI–SiO_2) nanocomposites were synthesized via in-situ oxidative polymerization assisted by ultrasonication to enhance filler dispersion and interfacial bonding. Different SiO_2 loadings (8 wt%, 18 wt%, and 28 wt%) and ultrasonication times were investigated to optimize conductivity and morphology. Structural analysis by X-ray Diffraction (XRD) and Fourier Transform Infrared Spectroscopy (FTIR) confirmed semi-crystalline ordering and strong interfacial interactions between PANI chains and SiO_2 nanoparticles. Field Emission Scanning Electron Microscopy (FESEM) and dynamic light scattering (DLS) revealed improved but heterogeneous dispersion of SiO_2 domains within the polymer matrix. Electrical conductivity and humidity sensing performance were optimal at 8 wt% SiO_2, while higher filler content led to reduced conductivity due to agglomeration. Humidity sensing tests demonstrated excellent sensitivity (>99.8%) across a wide relative humidity (11–93%), with stable and pronounced resistance responses attributed to hydrophilic Si–OH groups and enhanced proton hopping within the nanocomposite network. Compared with many reported conventional oxide-based sensors in the literature, the PANI–SiO_2 system offers potential advantages such as room-temperature operability and mechanical flexibility. These findings highlight the potential of ultrasonication-assisted PANI–SiO_2 nanocomposites for low-cost, high-performance humidity sensors in environmental monitoring and wearable applications.

Ultrasonication-assisted PANI–SiO_2 nanocomposite for high-sensitivity humidity sensing

Keywords: Polyaniline, silica, nanocomposites, ultrasonication, electrical conductivity, humidity sensing

Received: July 2025; Accepted: December 2025

Humidity, the measure of water vapor in a gas medium, is a critical parameter in a wide range of applications, including environmental monitoring, food packaging, pharmaceutical storage, semiconductor fabrication, and wearable healthcare devices. Humidity can be measured in two primary forms: absolute humidity and relative humidity (RH). The latter, due to its practical relevance, cost-efficiency, and ease of implementation, is widely used in industrial and commercial sensing systems [1, 2]. The presence of water molecules in ambient air, which are polar and reactive, makes humidity highly sensitive to even small temperature or pressure variations, affecting sensor response behaviour [3].

†Paper presented at the 1st International Conference on Chemical and Energy Engineering 2025 (ICChEE2025)

The design of humidity sensors has rapidly evolved with advances in materials science. Modern sensors are expected to offer high sensitivity, fast response and recovery times, good repeatability, minimal temperature dependence, and low production costs. Resistive-type humidity sensors, which operate by measuring electrical resistance variations due to water molecule adsorption and desorption, have gained wide attention for their simplicity and adaptability [4]. However, commercial sensors such as infrared or metal oxide types still suffer from drawbacks, including high power consumption, high-temperature operation, or material instability [5, 6].

In recent years, conductive polymers-especially polyaniline (PANI)-have garnered significant attention as promising candidates for humidity-sensitive materials. PANI is a pH-sensitive, π-conjugated polymer with excellent environmental stability, high processability, and facile synthesis [6]. Upon exposure to humidity, water molecules interact with the imine and amine groups in the polymer backbone, leading to protonation and a subsequent increase in electrical conductivity. Numerous studies have demonstrated the viability of PANI for humidity sensing. For example, Zeng et al. [6] reported that PANI nanofibers exhibit superior humidity response due to their high surface area and effective charge transport mechanisms. Similarly, Anisimov et al. [7] provided a comprehensive review of PANI-based composites, highlighting the material's tuneable response under varying relative humidity conditions and its biopolymer compatibility for flexible sensors. Furthermore, Nguyen et al. [8] synthesized PANI/SiO_2 nanocomposites and observed improved electrical and mechanical properties, showing that inorganic fillers enhanced water adsorption and proton hopping. Biswas et al. [9] even demonstrated a field-effect transistor sensor based on PANI with strong RH-dependent current modulation, confirming its integration potential in next-generation devices. Despite these advantages, pristine PANI suffers from drawbacks such as poor linearity, weak response at low RH levels, and aging effects during long-term operation. Therefore, research has increasingly focused on polymer–inorganic nanocomposites to overcome these limitations.

To overcome these challenges, researchers have focused on polymer–inorganic nanocomposites, where nanofillers enhance the polymer's physicochemical interaction with ambient humidity. Among various candidates, silicon SiO_2 is particularly attractive due to its high specific surface area, excellent chemical inertness, and strong hydrophilicity, which facilitate water molecule adsorption and interaction with the polymer matrix [4, 10]. Furthermore, SiO_2 nanoparticles can improve dispersion, mechanical strength, and interfacial charge transfer within the nanocomposite. Notably, the use of ultrasonication during synthesis has shown promise in promoting uniform nanoparticle distribution and enhancing the interfacial contact between organic and inorganic phases [11].

In this study, PANI–SiO_2 nanocomposites were synthesized via in-situ oxidative polymerization with ultrasonication treatment to facilitate dispersion and interfacial bonding. The synthesized material was subjected to comprehensive characterization including XRD, FTIR, FESEM, DLS and direct current (DC) conductivity testing. To evaluate its practical applicability, the nanocomposite was fabricated into pellet sensors and tested for humidity sensing performance using a sealed chamber with saturated salt solutions, covering a wide RH range from 11% to 93%. Resistance response, sensitivity, and RH-conductivity relationships were analysed to assess the nanocomposite's potential as a low-cost, high-performance humidity sensor.

EXPERIMENTAL SECTION

Materials and Chemicals

The following reagents were used in the synthesis of the PANI-SiO_2 nanocomposites: aniline, ammonium persulfate (APS), hydrochloric acid (HCl), SiO_2, methanol, and deionized water. All chemicals were of analytical grade and used without further purification.

Table 1. Compositions of PANI-SiO_2 nanocomposites.

S/NO	PANI (Wt %)	SiO_2 (Wt %)	PANI (g)	SiO_2 (g)
SiO_2-1	92%	8%	1.86	0.15
SiO_2-2	82%	18%	1.86	0.41
SiO_2-3	72%	28%	1.86	0.57

Figure 1. Macroscopic appearance of the synthesized PANI–SiO_2 nanocomposite. The blackish-green powder was stored in a sealed glass vial.

Synthesis of PANI-SiO_2 Nanocomposites

PANI–SiO_2 nanocomposites were synthesized via in-situ oxidative polymerization of aniline in acidic medium with ultrasonication assistance. Briefly, 0.2 M aniline (1.86 g) was dissolved in 100 mL of 1 M HCl, followed by the addition of SiO_2 nanoparticles at 8%, 18%, or 28% weight ratios relative to aniline as shown in Table 1. The selected SiO_2 weight percentages (8%, 18%, and 28%) were designed to investigate the effect of filler loading on electrical and humidity sensing performance, particularly near the expected percolation threshold. Prior studies have shown that polymer–oxide nanocomposites exhibit an optimal balance between electrical conductivity and sensing behaviour at moderate filler contents, typically between 10% and 25% [12, 13]. A low SiO_2 ratio (8 wt%) allows evaluation of baseline dispersion and minimal dielectric interference, while intermediate loading (18 wt%) targets the percolation zone where conductive and sensing properties are enhanced. The highest concentration (28 wt%) was chosen to observe the effect of excessive filler, which often results in reduced conductivity due to interruption of the polymer's charge transport pathways. This range allows a comprehensive assessment of how filler content influences composite structure and performance. The mixture was stirred thoroughly to achieve uniform dispersion. Separately, 5.70 g of APS was dissolved in 100 mL of 1 M HCl and slowly added to the aniline/SiO_2 dispersion under continuous stirring. Once the solution turned dark green, ultrasonication was applied using a probe-type device (UCD-2000, 50 Hz) at 25% power with pulse cycles (3 seconds on, 6 seconds off) for 20, 30, or 40 minutes. The resulting suspension was left overnight for complete polymerization, filtered, washed with deionized water and methanol, and dried at 70 °C for 5 hours. Figure 1 shows the macroscopic appearance of the synthesized PANI–SiO_2 nanocomposite.

Characterization Techniques

All characterization tests in this study—including conductivity, structural analysis, morphological imaging, particle size distribution, and humidity response—were conducted only on the synthesized PANI–SiO_2 nanocomposites. No separate characterization was performed for pristine PANI or SiO_2 alone, as the focus of this work was to evaluate the integrated properties of the composite system.

Electrical Conductivity Measurement

The DC electrical conductivity of the PANI–SiO_2 nanocomposites was measured using a standard four-point probe technique (ST2258C, Suzhou Jingge Electronics). Powder samples were compressed into circular pellets (10 mm diameter, 1 mm thickness) using a hydraulic press without any binders. Measurements were conducted at the pellet centre to ensure accuracy and uniformity. A constant current was applied through the outer probes, and the voltage drop across the inner probes was recorded to determine sheet resistance. All tests were performed at room temperature under ambient conditions. The electrical resistivity (ρ) was obtained from the instrument output, and conductivity (σ) was calculated as:

$$\sigma = \frac{1}{\rho} \tag{1}$$

The structural and morphological properties of the synthesized PANI–SiO_2 nanocomposites were investigated using multiple techniques.

XRD

XRD was performed on a Rigaku SmartLab diffractometer with Cu Kα radiation (λ = 1.5406 Å), operated at 40 kV and 30 mA, over a 2θ range of 3°–100° at 8.25°/min. Powdered samples were pressed onto glass holders to analyse crystallinity and phase composition.

FTIR

FTIR spectra of the PANI–SiO_2 nanocomposites were recorded using a PerkinElmer Frontier spectrometer in ATR mode over the range of 4000–650 cm^{-1}, with 4 cm^{-1} resolution. The test identified functional groups and possible interactions between PANI chains and SiO_2 particles in the composite.

FESEM

Surface morphology and particle distribution were observed using FESEM (Hitachi SU8000) at 5 kV after sputter-coating samples with gold. No separate imaging of pure SiO_2 or PANI was performed due to instrument time limitations and cost considerations.

DLS

Particle size distribution of the nanocomposites was analysed using an Anton Paar Litesizer 500. Approximately 2 mg of each composite sample was dispersed in deionized water, ultrasonicated, and measured to assess agglomeration and dispersion behaviour.

Humidity Sensing Performance

The humidity sensing performance of PANI–SiO_2 nanocomposites was evaluated using a sealed chamber containing saturated salt solutions to generate fixed relative humidity (RH) levels at 25 °C. Saturated solutions of lithium chloride (LiCl, ~11% RH), potassium acetate (CH_3COOK, ~20% RH), magnesium chloride ($MgCl_2$, ~40% RH), potassium carbonate (K_2CO_3, ~60% RH), sodium chloride (NaCl, ~75% RH), and potassium nitrate (KNO_3, ~93% RH) were used to establish controlled RH environments. The nanocomposite sensing layer was fabricated by directly depositing the polymer solution onto silver interdigitated electrodes via electrospinning using a laboratory-scale electrospinning apparatus (LS901, Nanolab Instruments, Malaysia). After drying, the sensors were connected via shielded cables to a digital multimeter (Keithley 2110) for resistance measurements. Readings were recorded after stabilization at each RH level. All measurements were conducted at room temperature (~25 °C), and each test was repeated three times to ensure reproducibility.

All experimental measurements, including electrical conductivity, particle size distribution, and humidity response, were conducted in triplicate to ensure reproducibility. The results are presented as mean values, and error bars indicate standard deviations. Basic statistical analysis was performed using Microsoft Excel to assess the consistency of replicate measurements. However, no advanced significance testing (e.g., ANOVA or t-test) was applied, as the study's primary focus was on trend evaluation rather than hypothesis-driven comparison among treatments.

RESULTS AND DISCUSSION

Electrical Conductivity

The electrical conductivity of PANI–SiO_2 nanocomposites was calculated based on resistivity data obtained through the four-probe method, with average values derived from 30-second measurements under 0.1 μA current. The results are summarized in Figure 2.

At 8 wt% SiO_2, the conductivity reached its maximum value at 20 min, decreased to 1.19×10^{-3} S/m at 20 min, and partially recovered to 1.45×10^{-3} S/m at 30 min. For the 18 wt% sample, conductivity remained relatively stable in the range of 1.16–1.51×10^{-3} S/m, suggesting a balance between filler dispersion and conductive network integrity. In contrast, the 28 wt% sample exhibited the lowest values overall, dropping to 0.89×10^{-3} S/m at 20 min, which is attributed to excessive insulating oxide disrupting the conjugated backbone. This non-monotonic behaviour aligns with previously reported observations in similar PANI–oxide systems, where a balance between conductive polymer and dielectric filler governs transport pathways [12, 13].

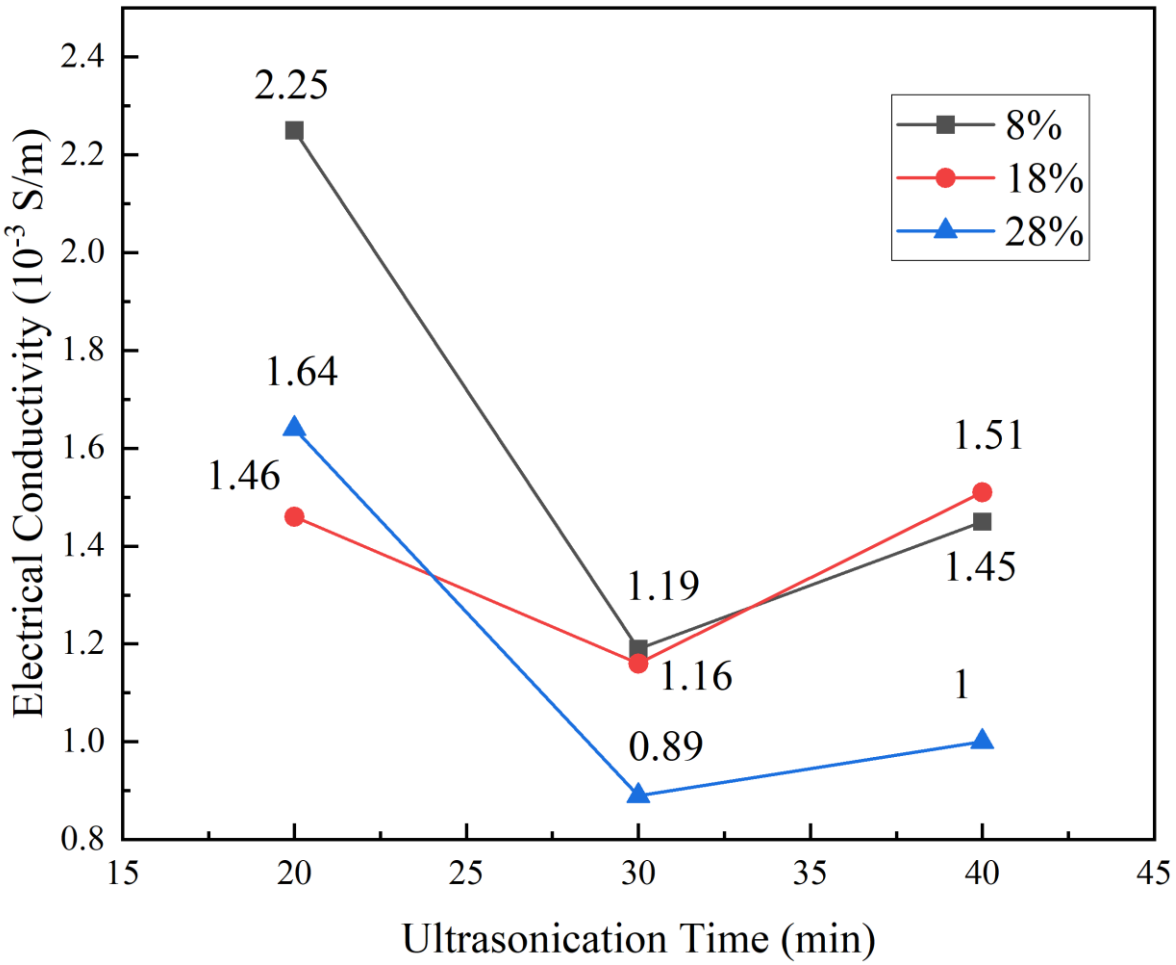

Figure 2. Electrical conductivity results of PANI-SiO_2 nanocomposites at concentrations of 8 wt%, 18 wt% and 28 wt%.

From the perspective of resistive-type humidity sensors, these conductivity results are significant. A higher baseline conductivity, as seen for the 8 wt% sample at 20 min, enhances sensitivity to small humidity variations by facilitating charge transport upon water adsorption. Meanwhile, the 18 wt% composition, though less conductive, shows greater stability across different ultrasonication times, which can contribute to reproducibility and long-term performance. Anisimov *et al*. [7] and Nguyen *et al*. [8] emphasized that moderate filler loading not only enhances electrical transport but also supports improved water adsorption via surface hydroxyl groups, which facilitate proton exchange mechanisms critical for humidity detection.

Overall, the interplay between conductive network integrity and dielectric filler dispersion plays a pivotal role in achieving high sensitivity and reliable performance in PANI-based humidity sensors. The conductivity findings herein provide a rational basis for selecting composition parameters in future sensor development [14, 15].

XRD Analysis

The XRD pattern of the PANI–SiO_2 nanocomposite (8 wt%) subjected to 20 minutes of ultrasonication is illustrated in Figure 3. The pattern exhibits characteristic peaks within the 2θ range of 10°–35°, with dominant reflections at approximately 15.2°, 20.3°, 25.1°, and 30.5°. The broad peak centred around 20.3° corresponds to the (020) plane of polyaniline, commonly associated with the periodic π–π stacking of the polymer chains in the emeraldine salt form, indicative of its semi-crystalline nature [16]. Meanwhile, sharper peaks near 25°–30° arise from the Si–O–Si networks of embedded SiO_2 nanoparticles, implying partial retention of short-range crystalline order within the SiO_2 phase [13].

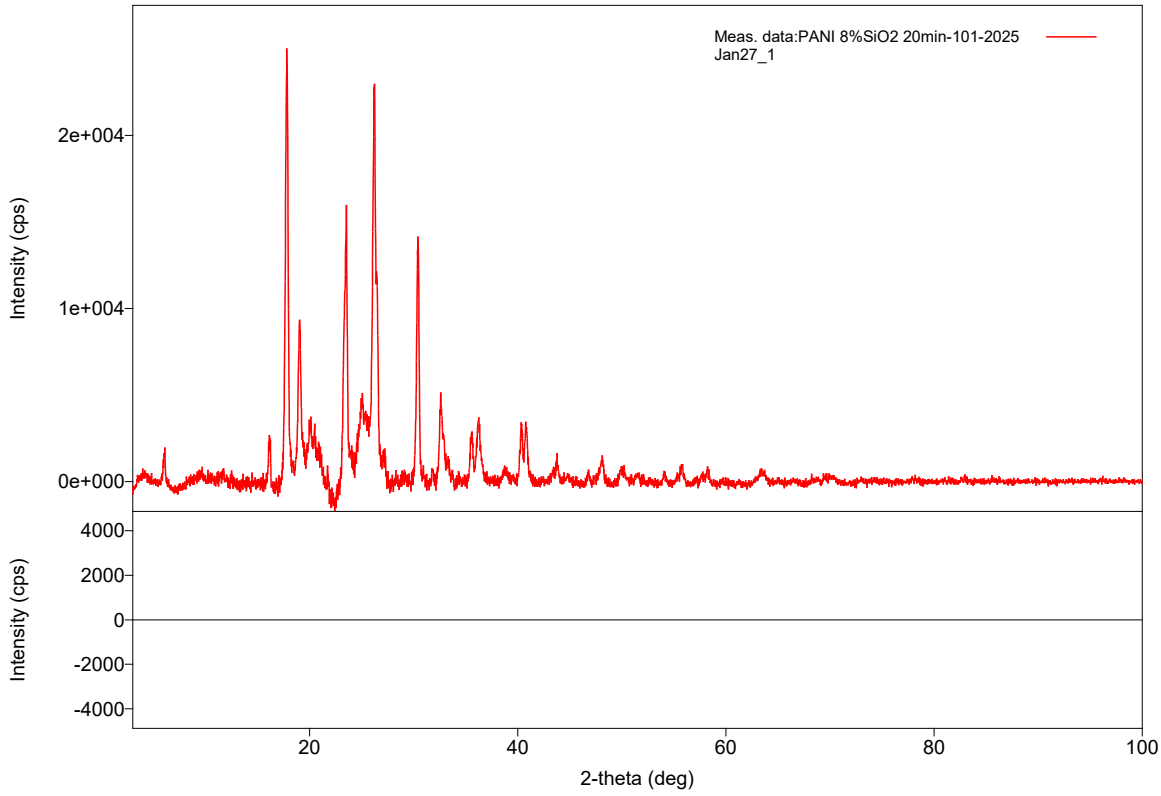

Figure 3. XRD spectra of 20min ultrasonication treated PANI-8 wt%SiO_2.

Compared with neat PANI, the incorporation of SiO_2 results in enhanced intensity and slight sharpening of certain diffraction peaks. This suggests that the inorganic filler contributes to local structural ordering and promotes better interfacial packing, which can support improved charge carrier pathways. Notably, no high-angle (>35°) crystalline peaks were observed, reaffirming that the material maintains its predominantly amorphous character beyond these primary stacking regions.

The application of ultrasonication (20 minutes) plays a pivotal role in achieving such structural refinement. It facilitates effective filler dispersion and interfacial adhesion, which aligns with literature reporting that moderate ultrasonication time improves nanocomposite homogeneity and enhances functional integration of filler particles [7, 17].

From a humidity sensor perspective, these structural features are of critical importance. The increased interfacial ordering between the PANI matrix and SiO_2 can promote better water adsorption and desorption kinetics due to the presence of more accessible surface sites and tailored free volume within the polymer network [18]. Additionally, the semi-crystalline morphology assists in balancing mechanical integrity and sorption responsiveness, both of which are essential in maintaining stable performance during repeated humidity cycling [19]. Studies have shown that nanocomposites with fine-tuned morphology and optimized filler distribution—such as observed here—exhibit superior sensitivity and lower hysteresis in humidity sensor applications [20, 21].

Furthermore, SiO_2 incorporation enhances hydrophilicity and increases available active sites due to its high surface area and polar surface chemistry, thereby improving sensor responsiveness and linearity across varying humidity levels [5]. Thus, the observed XRD features directly correlate with the nanocomposite's functional performance as a humidity sensor. Although direct XRD comparison with pristine PANI and pure SiO_2 was not performed in this study, key diffraction features were identified based on prior literature reports [10, 15]. For instance, the broad peak at ~20.3° corresponds to the (020) plane of PANI [15], while the sharper reflections near 25°–30° are consistent with the short-range crystalline order of amorphous SiO_2 [10]. These references provide a valid basis for interpreting the structural features of the composite material.

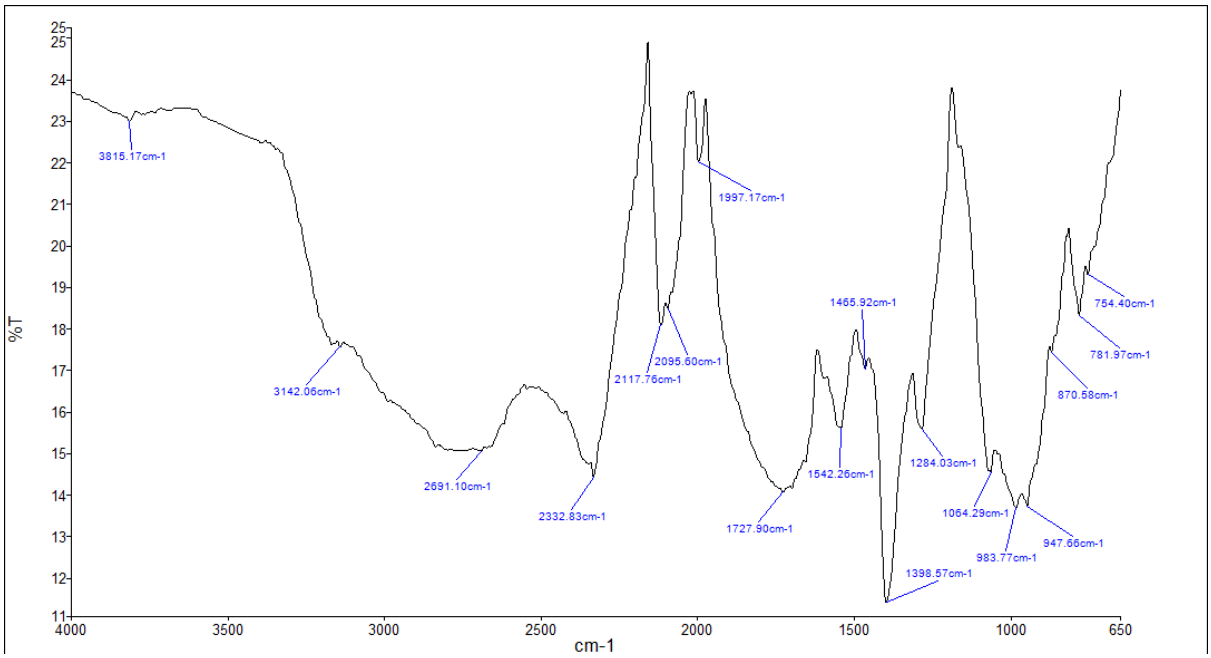

Figure 4. FTIR spectra of 20min ultrasonication treated PANI-8 wt%SiO_2.

FTIR Analysis

The FTIR spectrum of the PANI–SiO_2 nanocomposite (8 wt%) treated with 20 minutes of ultrasonication is illustrated in Figure 4. The spectrum clearly displays characteristic vibrational bands associated with the emeraldine salt form of polyaniline. Notably, the peaks at 1542 cm^{-1} and 1465 cm^{-1} correspond to the C=C stretching vibrations in quinoid and benzenoid rings, respectively, reflecting the presence of alternating conjugated segments that facilitate charge delocalization [16]. These are accompanied by bands in the 1240–1294 cm^{-1} range, attributed to C–N stretching and C–H in-plane bending vibrations in aromatic amine groups [7].

The 1398 cm^{-1} shoulder observed in the composite likely indicates subtle structural perturbations in the PANI backbone due to hydrogen bonding and electrostatic interactions with SiO_2 nanoparticles. Importantly, a broad absorption between 3142 cm^{-1} and 3815 cm^{-1} signifies O–H stretching, confirming the presence of hydrophilic surface hydroxyl groups contributed by SiO_2, which are known to promote water molecule adsorption during humidity sensing [22].

Additionally, absorption bands at 870 cm^{-1}, 781 cm^{-1}, and 754 cm^{-1} correspond to Si–O–Si symmetric stretching and bending modes, verifying the successful incorporation of SiO_2 into the polymer matrix [23]. The weak overtone-like band around 2117 cm^{-1} may be attributed to combination or overtone vibrations, often amplified in hybrid nanocomposites.

Crucially, the presence of both PANI and SiO_2 vibrational signatures, along with observable shifts in the quinoid and C–N bands, supports the existence of interfacial interactions between the two components. Such interactions, enhanced by ultrasonication, can induce reorganized chain conformations that increase water uptake affinity and promote proton hopping mechanisms during humidity exposure—mechanisms central to resistive-type humidity sensors [7, 24]. Prior research has established that these chemical modifications directly influence sensor responsiveness, stability, and linearity under varying RH conditions [23]. Due to the study's focus on composite behaviour, separate FTIR spectra for pristine PANI and SiO_2 were not recorded. However, the identification of characteristic bands—such as quinoid/benzenoid C=C stretches, Si–O–Si vibrations, and O–H groups—was guided by established literature values [11, 22], allowing reliable inference of interfacial interactions between components.

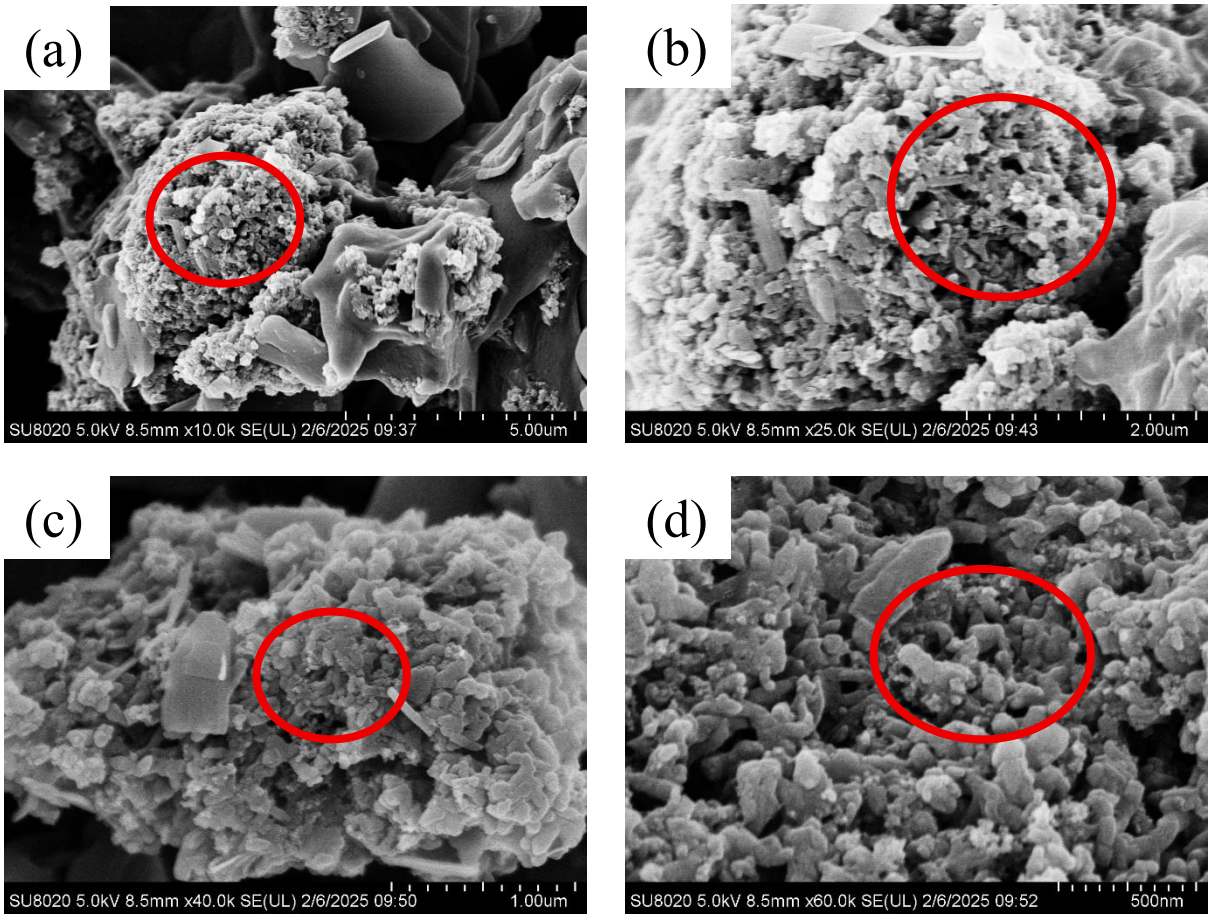

Figure 5. FESEM images of PANI–SiO_2 nanocomposites synthesized via ultrasonication (20 min), captured at increasing magnifications. Red circles indicate SiO_2-rich domains, inferred from morphology contrast and particle texture. (a) 5 µm, (b) 2 µm, (c) 1 µm, and (d) 500 nm.

FESEM & DLS

The surface morphology of the PANI–8 wt% SiO_2 nanocomposite (20 min ultrasonicated) is shown in Figure 5. At lower magnification [Figure 5(a)], the sample reveals irregularly shaped, agglomerated clusters with coarse granular features. These large clusters are composed of smaller particles embedded within the polymer matrix, suggesting incomplete deagglomeration at the micron scale. At higher magnification [Figure 5(b) and 5(c)], a more detailed particulate structure becomes evident. The SiO_2 nanoparticles appear well integrated but partially clustered, embedded in the polyaniline network. Plate-like structures observed throughout may correspond to larger PANI sheets or aggregated SiO_2 domains. At the nanoscale [Figure 5(d)], a relatively uniform dispersion of submicron particles can be seen, although local clustering remains. The ultrasonication treatment helped break up larger agglomerates, improving overall dispersion and interfacial contact, yet some interparticle aggregation persists—a common occurrence in hybrid systems due to Van der Waals and hydrogen bonding forces. These observations are consistent with previous reports, where moderate sonication improved nanofiller dispersion in polymer matrices but could not entirely eliminate aggregation [25, 26].

From the perspective of humidity sensing, the FESEM images provide valuable insights into structure–function relationships. The presence of SiO_2 nanoparticles within the PANI matrix introduces hydrophilic –OH groups at the surface, which act as active adsorption sites for water molecules. The heterogeneous morphology, with a combination of micron-scale clusters and submicron domains, creates a hierarchical porous network that enhances vapor diffusion and facilitates proton conduction pathways during sensing. Well-dispersed SiO_2 domains ensure increased surface area and fast response, whereas residual agglomerates may contribute to slower recovery times due to water retention within larger clusters. This duality is commonly reported in polymer–inorganic hybrids, where controlled dispersion directly governs sensitivity and stability [27, 28].

Furthermore, the interconnected granular structure observed here supports efficient charge transport through the conducting PANI backbone, which is crucial for resistance-type humidity sensors. Recent studies on PANI/oxide systems confirm that microstructural tailoring, particularly through ultrasonication or templating, can significantly boost sensor reproducibility and operational lifetime [29, 30]. Therefore, the FESEM analysis not only confirms the partial success of ultrasonication in dispersing SiO_2 but also highlights the importance of morphology optimization to maximize sensing efficiency in PANI–SiO_2 nanocomposites.

The particle size distribution of the PANI–8 wt% SiO_2 nanocomposite subjected to 20 minutes of ultrasonication was evaluated by DLS, and the results are shown in Figure 6. All three replicates revealed a consistent trimodal distribution with primary peaks in the 4.1–5.5 µm range, indicating partial agglomeration. The hydrodynamic diameters were measured as 4.67 µm, 6.03 µm, and 6.08 µm, with polydispersity indices (PDI) ranging from 0.259 to 0.291, suggesting moderate polydispersity. A secondary population of smaller particles was observed in the sub-micron range (0.30–0.79 µm), likely corresponding to well-dispersed SiO_2 domains or smaller PANI fragments. The presence of multiple peaks confirms the heterogeneous size distribution commonly found in hybrid polymer–inorganic systems. The ultrasonication treatment reduced agglomeration compared to non-sonicated samples (as reported by Kumar *et al*. [31]), yet residual clustering remains, likely due to strong interparticle interactions.

These micro- and submicron-scale clusters have direct implications for the humidity sensing performance of the nanocomposite. Larger PANI–SiO_2 aggregates reduce the effective surface area and hinder proton transport, while the smaller SiO_2-enriched domains provide hydrophilic adsorption sites that facilitate water uptake. Similar correlations between particle size distribution and humidity response have been reported for PANI–metal oxide hybrids, where reduced agglomeration enhanced sensitivity and response times [27, 32]. Optimizing the ultrasonication conditions to narrow the particle size distribution could further enhance the reproducibility and stability of the humidity response, consistent with trends reported in recent PANI/SiO_2-based sensors [29, 30]. Overall, the DLS findings not only corroborate SEM imaging but also highlight the structure–function relationship between particle dispersion and humidity sensing behaviour in PANI–SiO_2 nanocomposites.

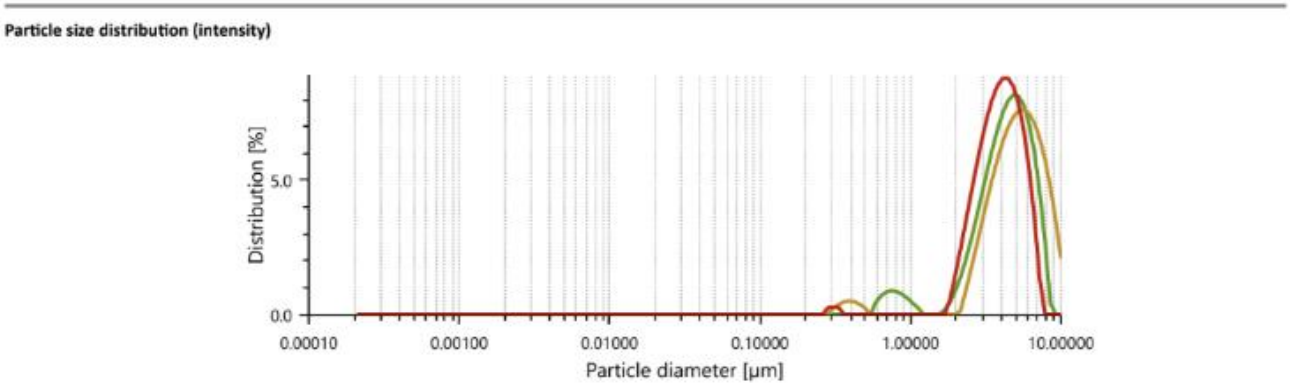

Measurements - Intensity

Index	Color	Hydrodyn. diam. [µm]	Polydisp. index [%]	Peak 1 [µm]	Peak 2 [µm]	Peak 3 [µm]	Transmittance [%]
1		4.674	29.1	4.648 (Intensity)	0.7981 (Intensity)	- (Intensity)	4.8
2		6.028	25.9	5.515 (Intensity)	0.3952 (Intensity)	- (Intensity)	5.1
3		6.083	27.2	4.119 (Intensity)	0.3075 (Intensity)	- (Intensity)	5.6

Figure 6. DLS analysis of 20min ultrasonication treated PANI-8 wt%SiO_2.

Humidity Sensing Behaviour

To investigate the effect of inorganic filler content, nanocomposites with three different SiO_2 loadings (8 wt%, 18 wt%, and 28 wt%) were synthesized and evaluated. The 8 wt% PANI–SiO_2 nanocomposite demonstrated the best sensing characteristics, including stable resistance response, higher sensitivity in the mid-RH range (40–75%), and minimal hysteresis. In contrast, the 18 wt% and 28 wt% samples exhibited reduced conductivity, likely due to excessive SiO_2 causing filler aggregation and disrupting the conductive pathways. As a result, the 8% composition was selected for in-depth structural and performance analysis in this study. The PANI–SiO_2 nanocomposite exhibited a pronounced and continuous resistance decrease in response to increasing relative humidity (RH), as illustrated in Figure 7. Starting from 6435.8 MΩ at 11% RH, the resistance fell significantly to 7.74 MΩ at 93% RH. Intermediate values such as 3077 MΩ (20% RH), 597 MΩ (40% RH), 115.8 MΩ (60% RH), and 33.86 MΩ (75% RH) demonstrate the sensor's consistent and nonlinear humidity responsiveness. The sensitivity (S) was calculated using the formula:

$$S = \frac{R_{low\ RH} - R_{high\ RH}}{R_{low\ RH}} \times 100\%$$

where R_{low} and R_{high} are the resistance values at 11% and 93% RH, respectively. The resulting sensitivity was approximately 99.88%, demonstrating the nanocomposite's excellent responsiveness to humidity variations.

This strong sensitivity is attributed to the synergistic behaviour between the conductive polymer matrix and the SiO_2 nanoparticles. Polyaniline exhibits variable electrical conductivity due to its doping level, which increases upon water molecule adsorption. The incorporation of SiO_2 enhances this effect by providing a hydrophilic surface rich in silanol groups (–Si–OH), which facilitates water uptake and intensifies protonation along the PANI backbone. As water molecules accumulate, they form conductive channels that support charge transport, resulting in a dramatic resistance decrease. These effects have been consistently reported in the literature, affirming that hydrogen bonding and surface hydroxylation play a crucial role in enhancing humidity sensitivity [33, 34].

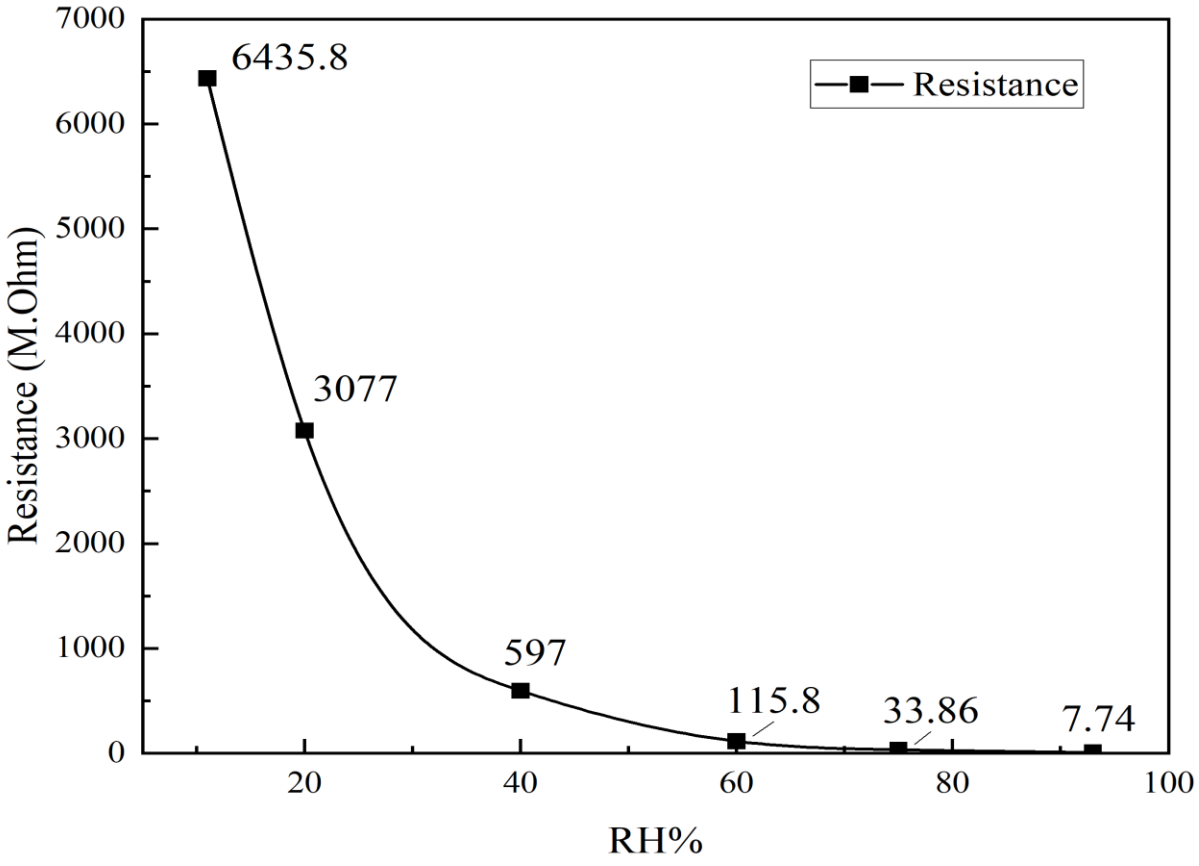

Figure 7. Change in resistance with relative humidity of PANI-SiO_2 with 20 min ultrasonication treatment. All data represent mean values from three replicate measurements. The variation was consistently low (standard deviation < 3%), indicating good reproducibility.

In this study, the sensing layer was fabricated by directly electrospinning the PANI–SiO_2 nanocomposite onto silver interdigitated electrodes, forming a nanofibrous and porous network. This structure ensures rapid adsorption, short diffusion pathways, and intimate contact between the sensing material and the electrode surface. Such architecture has been shown to promote fast response, stable signal output, and improved long-term performance in polymer–oxide humidity sensors [35, 36].

Compared with traditional metal oxide sensors or bulk PANI systems, the presented nanocomposite exhibits high sensitivity over a wide humidity range, with a resistance drop exceeding 99% between 11% and 93% RH under room temperature conditions. These results, in line with earlier studies, highlight the potential of PANI–SiO_2 hybrid systems for low-cost, flexible, and room-temperature humidity sensing in environmental monitoring, wearable electronics, and biomedical fields [9, 37].

CONCLUSION

This study presented a comprehensive evaluation of PANI–SiO_2 nanocomposites synthesized via in-situ oxidative polymerization with ultrasonication assistance. Among the compositions investigated, PANI-8 wt%SiO_2 nanocomposites treated with 20 minutes of ultrasonication demonstrated the most favourable combination of conductivity, morphology, and humidity sensitivity. These improvements are attributed to optimal filler dispersion, enhanced interfacial interaction, and structural reorganization of the PANI matrix promoted by controlled ultrasonication.

XRD and FTIR results confirmed semi-crystalline ordering and strong hydrogen bonding between the SiO_2 nanoparticles and PANI chains. FESEM and PSA analyses further revealed uniform particle dispersion and reduced aggregation, key for creating continuous charge transport pathways and ensuring stable sensor response. The conductivity results also aligned with typical percolation behaviour, where moderate oxide loading promotes electronic mobility through localized hopping and interfacial polarization [38-40].

The humidity sensing performance of the optimized PANI–SiO_2 nanocomposite showed exceptional sensitivity (>99.8%) over a broad RH range (11%–93%), with pronounced resistive response even at intermediate humidities (20%, 40%, 60%). The integration of electro spun nanofibrous architecture using silver interdigitated electrodes significantly contributed to this performance by increasing the active surface area and facilitating water molecule diffusion [41, 42]. These findings align with recent reports emphasizing the role of porous polymer–inorganic hybrids in enhancing low-power, room-temperature humidity detection [43].

Compared to traditional ceramic- or metal oxide-only humidity sensors, the PANI–SiO_2 system demonstrated high flexibility, rapid response, and low-temperature operability—traits desirable in applications such as wearable health monitors, intelligent packaging, and indoor environmental regulation [44]. Furthermore, the reproducibility of the sensor response and stability of the morphology under ambient conditions suggests strong promise for real-world integration.

Future work should consider the incorporation of additional nanofillers (e.g., graphene oxide, MXene) to further tailor the conductivity–sensitivity balance. Additionally, long-term cycling stability, response/recovery time quantification, and environmental cross-sensitivity (e.g., temperature, gas interference) merit investigation. The combination of controlled ultrasonication and nanofiber fabrication opens up scalable pathways toward miniaturized, flexible humidity sensing platforms that align with emerging demands in Internet of Things (IoT) and biomedical diagnostics [45].

ACKNOWLEDGEMENT

The authors would like to express their sincere gratitude to the Institute of Oil & Gas (IFOG), Universiti Teknologi Malaysia, for providing access to experimental facilities and instrumentation. Special thanks are extended to the corresponding supervisor and colleagues at IFOG whose support and assistance were invaluable to the successful completion of this work.

The authors declare that they have no conflict of interest.

REFERENCE

1. Yakubu, I. S. A., Muhammad, U. and A'isha, A. M. (2018) Humidity sensing study of polyaniline/copper oxide nanocomposites, *International Journal of Advanced Academic Research Sciences: Technology & Engineering*, **4(5)**, 49–61.

2. Farahani, H., Wagiran, R. and Hamidon, M. N. (2014) Humidity sensors principle, mechanism, and fabrication technologies: a comprehensive review. *Sensors*, **14(5)**, 7881–7939.

3. Sikarwar, S. and Yadav, B. (2015) Opto-electronic humidity sensor: A review. *Sensors and Actuators A: Physical*, 233, 54–70.

4. Gu, W., Zhang, H., Chen, C. and Zhang, J. (2022) Study on the design of ZnO/PANI composites and the mechanism of enhanced humidity sensing properties. *Current Applied Physics*, **34**, 112–121.

5. Chen, Z. and Lu, C. (2005) Humidity sensors: a review of materials and mechanisms. *Sensor Letters*, **3(4)**, 274–295.

6. Zeng, F. -W., Liu, X. -X., Diamond, D. and Lau, K. T. (2010) Humidity sensors based on polyaniline nanofibres. *Sensors and Actuators B: Chemical*, **143(2)**, 530–534.

7. Anisimov, Y. A., Evitts, R. W., Cree, D. E. and Wilson, L. D. (2021) Polyaniline/biopolymer composite systems for humidity sensor applications: A review. *Polymers*, **13(16)**, 2722.

8. Nguyen, A. S., Nguyen, T. D., Thai, T. T., Trinh, A. T., Pham, G. V., Thai, H., Tran, D. L., To, T. X. H. and Nguyen, D. T. (2020) Synthesis of conducting PANi/SiO2 nanocomposites and their effect on electrical and mechanical properties of antistatic waterborne epoxy coating. *Journal of Coatings Technology and Research*, **17(2)**, 361–370.

9. Biswas, M., Dey, A. and Sarkar, S. K. (2022) Polyaniline based field effect transistor for humidity sensor. *Silicon*, **14(14)**, 8919–8925.

10. Nunes, D., Pimentel, A., Gonçalves, A., Pereira, S., Branquinho, R., Barquinha, P., Fortunato, E. and Martins, R. (2019) Metal oxide nanostructures for sensor applications. *Semiconductor Science and Technology*, **34(4)**, 043001.

11. Pang, A. L., Arsad, A. and Ahmadipour, M. (2021) Synthesis and factor affecting on the conductivity of polypyrrole: a short review. *Polymers for Advanced Technologies*, **32(4)**, 1428–1454.

12. Pang, Z., Yu, J., Li, D., Nie, Q., Zhang, J. and Wei, Q. (2018) Free-standing TiO2–SiO2/PANI composite nanofibers for ammonia sensors. *Journal of Materials Science: Materials in Electronics*, **29(5)**, 3576–3583.

13. Horbenko, Y. Y., Tsizh, B., Aksimentyeva, O., Olenych, I., Bogatyrev, V. and Dzeryn, M. (2019) Effect of the modified silica on the conductivity and sensory properties of polyaniline nano-composites. *Науковий вісник Львівського національного університету ветеринарної медицини та біотехнологій імені СЗ Гжицького*, **21(91 (2))**, 29–37.

14. Korotcenkov, G., Simonenko, N. P., Simonenko, E. P., Sysoev, V. V. and Brinzari, V. (2023) Based Humidity Sensors as Promising Flexible Devices, State of the Art, Part 2: Humidity-Sensor Performances. *Nanomaterials*, **13(8)**, 1381.

15. Wu, J., Wu, Z., Tao, K., Liu, C., Yang, B. -R., Xie, X. and Lu, X. (2019) Rapid-response, reversible and flexible humidity sensing platform using a hydrophobic and porous substrate. *Journal of Materials Chemistry B*, **7(12)**, 2063–2073.

16. Stejskal, J. and Gilbert, R. (2002) Polyaniline. Preparation of a conducting polymer (IUPAC technical report). *Pure and Applied Chemistry*, **74(5)**, 857–867.

17. Singh, P. and Shukla, S. (2020) Structurally optimized cupric oxide/polyaniline nanocomposites for efficient humidity sensing. *Surfaces and Interfaces*, **18**, 100410.

18. Nie, Q., Pang, Z., Li, D., Zhou, H., Huang, F., Cai, Y. and Wei, Q. (2018) Facile fabrication of flexible SiO2/PANI nanofibers for ammonia gas sensing at room temperature. *Colloids and Surfaces A: Physicochemical and Engineering Aspects*, **537**, 532–539.

19. Anisimov, I. A., Evitts, R. W., Cree, D. E. and Wilson, L. D. (2022) Renewable hybrid biopolymer/polyaniline composites for humidity sensing. *ACS Applied Polymer Materials*, **4(10)**, 7204–7216.

20. Li, X., Cai, F., Cao, J., Fu, N., Dong, Z., Long, N., Zhao, J. and Yao, Y. (2024) Graphene oxide/cellulose nanofiber-based capacitive humidity sensor with high sensitivity. *Sensors and Actuators A: Physical*, **368**, 115064.

21. Nazemi, H., Joseph, A., Park, J. and Emadi, A. (2019) Advanced micro-and nano-gas sensor technology: A review. *Sensors*, **19(6)**, 1285.

22. Chen, Z., Bao, Z., Song, Y., Yang, S. and Yin, X. (2025) Review on Solvent-Free Nanofluids in Fibers: Progress, Applications, and Prospects. *ACS Applied Polymer Materials*.

23. Pasalwad, K. A., Baby, N., Edjenguele, A., Sadhasivam, S., Palanisamy, G., Magdum, S. S., Thangarasu, S. and Oh, T. H. (2025) Progress on polymer-based materials and composites for humidity sensors applications: Materials aspects to sensor performances. *Journal of Materials Chemistry A*.

24. Boublia, A. (2024) Modeling and elaboration of multifunctional and ecofriendly nanocomposite materials based on polyaniline and functionalized graphene.

25. Soman, V., Vishwakarma, K. and Poddar, M. K. (2023) Ultrasound assisted synthesis of polymer nanocomposites: a review. *Journal of Polymer Research*, **30(11)**, 406.

26. Zahid, M., Anum, R., Siddique, S., Shakir, H. F. and Rehan, Z. (2023) Polyaniline-based nanocomposites for electromagnetic interference shielding applications: A review. *Journal of Thermoplastic Composite Materials*, **36(4)**, 1717–1761.

27. Al-Hartomy, O. A., Khasim, S., Roy, A. and Pasha, A. (2019) Highly conductive polyaniline/graphene nano-platelet composite sensor towards detection of toluene and benzene gases. *Applied Physics A*, **125(1)**, 12.

28. Supardi, Z. Synthesis of PANi-SiO2 Nanocomposite with In-Situ Polymerization Method: Nanoparticle Silica (NPS) Amorphous and Crystalline Phase.

29. Simotwo, S. K. (2017) Polyaniline Based Nanofibers for Energy Storage and Conversion Devices, Drexel University.

30. Tejwani, A., Sonkar, U., Shrivas, K., Tandey, K., Karbhal, I., Deb, M. K. and Pervez, S. (2025) Differential pulse voltametric detection of dopamine using polyaniline-functionalized graphene oxide/silica nanocomposite for point-of-care diagnostics. *RSC Advances*, **15(20)**, 15870–15878.

31. Kumar, P., Narayan Maiti, U., Sikdar, A., Kumar Das, T., Kumar, A. and Sudarsan, V. (2019) Recent advances in polymer and polymer composites for electromagnetic interference shielding: review and future prospects. *Polymer Reviews*, **59(4)**, 687–738.

32. Mezan, S. O., Hello, K. M., Jabbar, A. H., Hamzah, M. Q., Tuama, A., Roslan, M. and Agam, M. A. (2020) A review on synthesis of conducting with polyaniline rice husk ash silica nanocomposites and application. *International Journal of Psychosocial Rehabilitation*, **24(03)**.

33. Malhotra, B., Saxena, V., Gambhir, A., Singhal, R., Annapoorni, S. and Mukhopadhyay, A. (2001) 13 Conducting Polymers in Molecular Electronics. *Handbook of Polymers in Electronics*, **393**.

34. Ali, T. and Shah, M. (2021) Processing and optical characterization of ultra-sensitive humidity and pressure sensors based on polyaniline/holmium oxide hybrid nanocomposites. *Sensors and Actuators A: Physical*, **331**, 113040.

35. Ghayempour, S., Mazloum-Ardakani, M. and Dehghan-Manshadi, H. (2024) In *Semiconducting Fibers*, eds. *CRC Press*.

36. Wu, S. -X. and Li, G. -R. (2025) Recent Progress in Polyaniline-based Catalysts for Electrochemical Energy Conversion. *Nanoscale*.

37. Sharma, S., Sudhakara, P., Omran, A. A. B., Singh, J. and Ilyas, R. (2021) Recent trends and developments in conducting polymer nanocomposites for multifunctional applications. *Polymers*, **13(17)**, 2898.

38. Madhavan, R. (2025) Manufacturing of nanomaterial composites and flexible electronic devices with record high performance for human-technology design, human–computer interaction, biomedical sensing and soft robotics. *New Journal of Chemistry*, **49(5)**, 1700–1717.

39. Mallick, S. A. (2021) Polymer nanocomposite based humidity sensor.

40. Vinodhini, S. and Xavier, J. R. (2025) Recent progress in graphene-based nanocomposites for enhanced energy storage and corrosion protection. *Journal of Materials Science*, 1–43.

41. Zu, Y., Duan, Z., Yuan, Z., Jiang, Y. and Tai, H. (2024) Electrospun nanofiber-based humidity sensors: materials, devices, and emerging applications. *Journal of Materials Chemistry A*, **12(40)**, 27157–27179.

42. Anisimov, Y. A. (2022) Polyaniline/biopolymer composites for moisture detection and their electromechanical properties. *University of Saskatchewan*.

43. Liu, L., Fei, T., Guan, X., Lin, X., Zhao, H. and Zhang, T. (2020) Room temperature ammonia gas sensor based on ionic conductive biomass hydrogels. *Sensors and Actuators B: Chemical*, **320**, 128318.

44. Ma, Y., Li, W., Zhang, W., Kong, L., Yu, C., Tang, C., Zhu, Z., Chen, Y. and Jiang, L. (2024) Bioinspired multi-scale interface design for wet gas sensing based on rational water management. *Materials Horizons*, **11(17)**, 3996–4014.

45. Yuan, Z. and Shen, G. (2023) Materials and device architecture towards a multimodal electronic skin. *Materials Today*, **64**, 165–179.